Heavy ion cratering of gold

S. E. Donnelly* and R. C. Birtcher
Materials Science Division, Argonne National Laboratory, Argonne, Illinois 60439
(Received 14 November 1996; revised manuscript received 14 July 1997)

Irradiation of gold films with Xe ions in the energy range 50–400 keV has been monitored using *in situ* transmission electron microscopy. Craters are produced and annihilated on the irradiated surface at all ion energies studied. Approximately 2–5% of impinging ions in the energy range 50–400 keV produce craters with sizes as large as 12 nm for the higher-energy irradiations. Crater annihilation occurs in discrete steps, due to subsequent ion impacts, or by annealing in a continuous manner due to surface diffusion processes. Crater creation results from flow associated with near surface cascades. Discrete crater annihilation results from plastic flow induced by ion impacts, including those that do not themselves leave a crater, and annealing that may occur during the quenching phase of cascade thermal spikes. [S0163-1829(97)07046-X]

INTRODUCTION

The interaction of energetic ions with solid surfaces has been studied for more than 40 years and for many combinations of ion and solid the energy deposition process is reasonably well known and understood. In particular, when the individual collisions in the cascade can be regarded as simple, independent binary events, linear transport theory provides a reasonable description and yields parameters such as the sputtering yield that are in moderately good agreement with measurement. However, when the projectile mass and/or the atomic mass of the substrate are large, the mean free path between recoil collisions is on the order of one atomic spacing, and a highly disturbed volume known as an atomic displacement spike or energy spike is created.[1,2] In this case, the assumptions of the linear cascade model break down. The energy density in the spike corresponds to temperatures well above the melting or perhaps even the vaporization temperature of most materials.

Effects attributed to spike processes have been observed for heavy-ion and molecular ion bombardment of a number of materials.[3–6] In a recent publication, the present authors and colleagues carried out heavy-ion irradiation of gold *in situ* in a TEM in order to examine the effects of post-irradiation on helium gas bubbles in gold foils.[7] Both the disappearance and motion of bubbles appeared to result from spike effects. In a second publication, the present authors reported on the production of holes in very thin TEM gold foils as a result of single-ion impacts.[8]

The present work reports on *in situ* TEM observations of gold during heavy-ion irradiation. This work centers on the formation of small craters and their subsequent annihilation both by irradiation induced processes. Observation of craters following heavy-ion irradiation of gold was reported by Merkle and Jäger[3] and led to conclusions concerning both the contribution of spike effects to the overall sputtering yield and the mechanism responsible for crater formation. The *in situ* irradiation facility used in the present work has enabled us to video record, at high magnification, both the appearance and disappearance of craters during continued irradiation. This has allowed identification of surface flow processes rather than simply the ejection of material as being responsible for crater formation.

EXPERIMENTAL

Ion irradiations were carried out in a Hitachi H-9000 TEM operating at 300 keV at the IVEM/Accelerator Facility located at Argonne National Laboratory.[9] In the IVEM/Accelerator Facility, the ion beam is oriented 30° from the microscope axis, and the specimen was tilted 15° towards the ion beam so that both ions and electrons were incident on the specimen at 15° to the foil normal. Specimens were irradiated with Xe^+ ions at energies of 50, 200, or 400 keV at dose rates between 1 and 25 10^{10} ions/cm^2/s. Au films, 62 ± 5 nm thick with a $\langle 100 \rangle$ surface normal, were made by thermal evaporation of 99.999 at. % pure starting material onto NaCl at a temperature of 350 °C. Small pieces of Au film were floated off the NaCl on a water/alcohol mixture and picked up on either Au or Cu TEM grids.

Surface features were made visible in the TEM by defocusing the objective lens of the microscope (typically ≈ 1000 nm of underfocus). The phase contrast generates a Fresnel fringe around the feature even though little or no thickness contrast is discernible at focus. In underfocus, craters appear white surrounded by a dark fringe whereas particles on the surface appear dark surrounded by a light fringe. In addition to normal photographic recording made during interruptions of the irradiations, images from a Gatan 622 video camera and image-intensification system were continuously viewed with total magnifications of approximately 2 million, and recorded during irradiation on video tape with a time resolution of 1/30th s (a single video frame).

The possibility that craters may be created by the emission of large fragments was examined by collection of all sputtered Au atoms on a thin amorphous carbon foil 20 nm in thickness placed approximately 40 μm from either in front of or behind the irradiated gold film. This allowed the TEM to be focused on the carbon foil in order to detect the arrival of gold clusters without interference from the image of the Au foil. The resolution was sufficient to detect particles 1 nm in diameter.

RESULTS

Figure 1 shows images that have been digitized from video recordings made without interruption of continuous

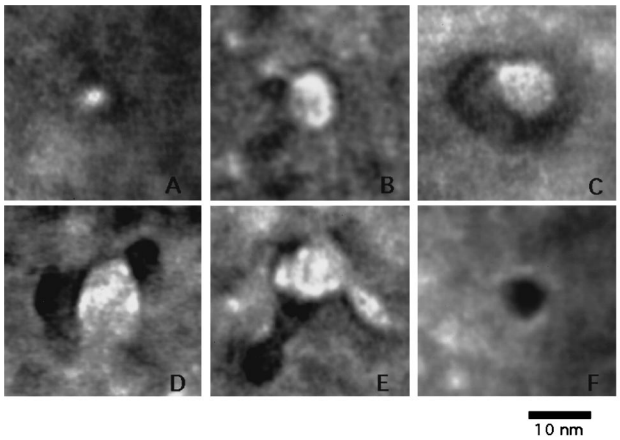

FIG. 1. Images (digitized from video recordings) resulting from single Xe ion impacts at (a) 50 keV, (b) 200 keV, and (c), (d), and (e) 400 keV Xe ions, (f) an isolated particle which appeared on the surface (between video frames) during irradiation with 400 keV Xe ions.

irradiations at room temperature. The craters visible are similar to those reported for Au irradiated with Br^+ and Br^{2+} ions.[3] Each crater occurred between video frames as the result of a single ion impact. Unlike our Xe irradiation of very thin bulk Au specimens,[8] no holes were produced by ions at any of the energies studied. Figure 1(a), recorded during a 50 keV Xe irradiation, shows a small crater that is typical of small craters observed for irradiations at all three energies studied. Figure 1(b) is a somewhat larger faceted crater, created by a 200 keV Xe ion, which has impacted close to pre-existing small craters. The craters in Figs. 1(c)–1(e) were all formed by 400 keV Xe ions and in each case, material is deposited on the surface concomitantly with crater formation. In Fig. 1(c), a faceted crater is surrounded by a faceted island. In Fig. 1(d), a two-part ''lid'' appears to have been ejected from the crater. Such lids were not observed during 50 keV irradiations. The contrast in Fig. 1(e) is consistent with a faceted crater and a quenched droplet of molten material that has been ejected on ion impact. (The light contrast to the right of this crater is the remnant of a pre-existing crater). If it is assumed that the expelled material in this case has cylindrical symmetry, then it contains approximately 20 000 gold atoms. If all the material in this droplet came from the adjacent crater, the crater would be approximately 4 nm deep. On this basis, the largest craters could involve as many as 40 000 gold atoms. Finally, Fig. 1(f) shows a particle on the surface that has appeared between successive video frames with no associated crater within a field of view approximately six times the area shown. A statistical analysis of more than 200 craters reveals that the mean crater area increases from 14 nm^2 at 50 keV to 32 nm^2 at 200 keV. For 200 and 400 keV there is no statistically significant difference in mean crater area (32 and 34 nm^2, respectively). The craters that remained on the Au surface at the end of an irradiation were stable at room temperature for periods longer than several months but disappeared slowly at a temperature of 440 K. This consistent with thermal recovery by surface diffusion.[10]

The emission of clusters of atoms under ion bombardment has been observed in computer simulations of ion impacts at

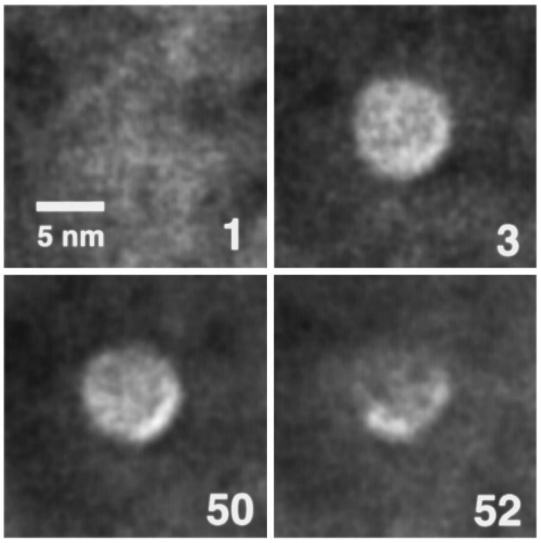

FIG. 2. The creation and annihilation of a crater as a result of impacts of individual 400 keV Xe ions. The numbers are video frame numbers (i.e., time steps in units of 1/30 s).

energies of 5 keV and below.[11] Although, in the simulations, cluster sizes were typically between 5 and 20 atoms, the significantly higher energy used in our experiments might be expected to give rise to somewhat larger clusters. To determine if this process occurs, sputtered material was collected on a 20 nm thick amorphous carbon foil placed either in front of or behind the gold film. Nucleation, clustering and growth of a sputter-deposited gold film on the carbon was observed, however cluster arrival was almost never observed. Specifically, for the 400 keV irradiation when the catcher foil was in front of a Au specimen mounted on a Au TEM grid, two particles (one ≈ 5 nm and the other < 2 nm in diameter) were observed in an area of 110×85 nm during an irradiation to a total dose of 8×10^{14} ions/cm^2. A crude estimate of the probability of cluster emission by a 400 keV ion is $\approx 3 \times 10^{-5}$ particles/ion corresponding to approximately one particles per 2000 craters. Crater formation is thus not, in general, accompanied by the ejection of crater-sized particles.

The static images give an incomplete recording of crater formation. The ''live'' image during continuous irradiation reveals a rapidly changing crater population with approximately seven craters in the field of view (110 nm$\times$85 nm) at any time. At the dose rate of 2.4×10^{11} ions/cm^2/s, statistically, there is one ion impact per second on the area of each segment of Fig. 1. The efficiency of crater creation ranges from 2–5 % implying that the majority of ion impacts annihilate craters without creating new ones. The ''life cycle'' of a crater at room temperature is illustrated in Fig. 2. A discrete change occurring between video frames is clearly the result of a single ion impact. To improve picture clarity by increasing the signal to noise ratio, each image consists of an average of four video frames taken before and after a discontinuous change. Figure 2 shows a crater ≈ 7.5 nm in diameter formed as a result of a single 400 keV Xe ion impact. The crater is partially faceted and remains essentially unchanged for 50 video frames (≈ 1.6 s) after which time a discrete event causes flow of material into the crater resulting in its partial obliteration. A few seconds later (not shown), the re-

maining contrast disappears in a second discrete event. Note that, in this particular case, no new crater was observed to form within the field of view (approximately six times the area shown) at the moment that the crater was filled in. However, in other cases, material expelled during the creation of a crater is seen to fill in a second nearby crater.

Under steady-state irradiation at room temperature, at a dose rate of 2.4×10^{11} ions/cm^2/s, craters have a lifetime in the range 1–12 s at all three ion energies studied. Small craters are generally annihilated in a single discrete event whereas larger craters disappear in two or more steps. Lifetime measurements on 14 craters with a mean diameter of 4.4. nm yield a mean lifetime of 4.9 s for craters annihilated in a single step. With the assumption that all ion impacts are capable of annihilating existing craters, the Xe ion has an annihilation cross section for small craters of approximately 85 nm^2, i.e., an ion impact within a radius of approximately 5 nm of the center of a small crater will annihilate the crater.

DISCUSSION

The major effect of heavy-ion irradiation of Au, in addition to the sputtering of material, is the creation of craters and the flow of material on the surface. Flow resulting from single-ion impacts has been reported in a recent paper[8] in which we observed the formation of holes through a thin gold TEM foil as a result of a pulsed, localized flow produced by individual ions impacts. Before beginning the discussion it is useful to summarize the present experimental findings:

(i) Single xenon ions impacting on a gold film form craters, sometimes clearly faceted, $\approx2-10$ nm in diameter at a rate of 0.02–0.05 craters/ion for ions with energies in the range 50–400 keV. The craters appear on the rear surface when the ions are capable of reaching that surface.

(ii) Occasionally, a ''lid,'' particle or ''droplet'' is associated with the creation of a large crater.

(iii) A particle, sometimes faceted, occasionally appears on the surface without the formation of a nearby crater.

(iv) Craters and particles are thermally stable at room temperature but unstable under continued irradiation. Material ejected from a newly formed crater is sometimes observed to directly annihilate a neighboring crater. An ion impact can annihilate a small crater or a reduce the diameter of a large crater. The cross section for annihilation of small craters is 85 nm^2.

The dynamics of crater creation and annihilation can be described by a simple rate theory. If N is the number of craters per unit area, P_c is the probability that an ion will form a crater, and σ_a is the cross section for crater annihilation by a subsequent cascade, then the change, δN, in the number of craters per unit area caused by the arrival of $\phi\delta t$ ions per unit area, is given by

$$\delta N = P_c\phi\delta t - N\sigma_a\phi\delta t, \tag{1}$$

which on integration yields

$$N=\left(\frac{P_c}{\sigma_a}\right)\{1-e^{-\sigma_a\phi t}\}. \tag{2}$$

Thus, after a transient phase, the number of craters per unit area is given by the ratio P_c/σ_a. At our highest observed creation rate (for 400 keV Xe irradiations), the values given for creation probability, 0.05, and annihilation cross section, 85 nm^2, yield a steady-state concentration of approximately seven craters in the field of view on the video monitor of 110×85 nm^2. This is an important point, as it implies that post-irradiation *ex situ* examinations carried out by Merkle and Jäger,[3] in which craters on a gold surface were assumed to accumulate without annihilation during the irradiation, significantly underestimated the actual number of crater creation events.

Although linear transport theory cannot describe the dense cascades created in Au, it is useful in estimating the spatial distribution of the energy deposition. The energy deposited in damage by Xe ions incident on gold has been calculated using the Monte Carlo program TRIM 96.[12] A Xe ion, with any of the three energies studied, deposits most of its energy in approximately spherical volumes between 10 and 20 nm in diameter. Although, not every atom in this volume is involved in the ballistic cascade, prompt processes result in the distribution of the energy throughout the cascade volume. Within $\approx10^{-11}$ s of ion impact, atoms within the cascade volume will have an average energy E of approximately 2 eV. Such an energy would result in melting and a 11% free volume expansion.

The effect of a localized energy deposition will depend upon its position relative to the specimen surfaces. If the cascade volume is many atomic layers from a surface, there will be a confined pressure spike. Assuming for simplicity that the kinetic theory of gases applies, the resulting pressure, P_{spike}, is estimated to be

$$P_{\text{spike}}=(2/3)NE. \tag{3}$$

For $E=2$ eV this yields a pressure of approximately 13 GPa. Similar conclusions concerning pressure have been reported by Averback *et al.* based on molecular dynamics (MD) simulations of a 10 keV spike in gold.[13] In their work, pressures in the range 5–8 GPa were observed to exist at the core of a very small spike from 0.65 to 4.9 ps following ion impact. A pressure spike of sufficient duration may be expected to result in the punching of a dislocation loop when

$$P_{\text{spike}}>\mu b/R, \tag{4}$$

where μ is the shear modulus of the gold, b is the Burgers vector of the loop, and R its radius (assumed to be the radius of the spike).[14] On the basis of this simple description, a spike 5 nm in diameter will punch out loops for pressures in excess of 3 GPA; a significantly lower value than predicted by simply considering the theoretical shear modulus.[3] Since this value is lower than the calculated spike pressure from either MD simulation or ideal gas considerations, loops generation can be expected. The final defect configuration predicted by this simple model, will be a vacancy-rich (formerly molten) core surrounded by punched-out, interstitial-type dislocation loops. This description is almost indistinguishable from the classic spike configuration described by

Brinkman[1,2] or the picture that has emerged from more recent MD simulations.[15] The essential difference, however, is that in the current model, interstitial loops are created directly rather than by the agglomeration of individual interstitial atoms. The appearance of an isolated particle may result from either the punching out of dislocation loops to the surface or the complete ejection of a solid plug that comes to rest at some distance from its crater.

Unlike the confined spike, the hot zone of a cascade close to a surface is able to expand freely in one direction. A likely consequence of the sudden melting of this volume of material, with its concomitant volume change of 11%, is an explosive funneling of gold atoms to the surface in a manner similar to that observed by Averback *et al.* in molecular-dynamics simulations of gold ions impacting on gold.[13] We believe that the features shown in Fig. 1(c) and 1(e) were formed in this way. In particular, features such as that shown in Fig. 1(e) provide strong evidence that surface spikes can result in a melting of gold. If the molten core of a spike does not directly erupt through the surface, the high localized pressure may result in the ejection of a plug of solid material which then permits the subsequent explosive flow of molten gold out of the crater onto the surface. We believe that this is the origin of the craters with associated lids or mounds as illustrated in Fig. 1(d). Material expelled from a new crater may flow across the surface and annihilate a nearby pre-existing crater. It is important to note that, on average, insufficient energy per atom is available to overcome the surface binding energy of 3.8 eV and that the majority of gold atoms will therefore remain on the surface.

Although the model accounts for experimentally observed items (i)–(iii) above, it does not provide an explanation for the efficient annihilation of craters by subsequent ion impacts [item (iv)]. While material ejected from the small percentage of spikes that occur at a surface may result in the direct annihilation of nearby pre-existing craters, this is not the case for the majority of subsurface spikes. We speculate that during the quenching phase of these spikes, irradiation stimulated surface atom mobility of previously ejected material and crater edges combined with defect fluxes to the surface leads to the annihilation of craters and particles. Similarly, the faceting of craters and particles, which may be irregular when created, occurs due to irradiation stimulated surface diffusion processes. These processes go to completion during the time required to record one video frame (1/30 s) so that all observed craters are the result of both the creation and subsequent annealing processes taking place during the quenching phase of the spike as well as any diffusion processes that go to completion at room temperature on a time scale of $\approx 1/30$ s.

CONCLUSIONS

Craters are continuously created and annihilated on the surface of gold during room-temperature irradiation with xenon ions in the energy range of 50–400 keV. *In situ* observations demonstrate that individual ion impacts are responsible for both processes, and that structures are stable at room temperature when irradiation ceases. The efficiency of crater production is $\approx 0.02-0.05$ craters per ion and the cross section for crater annihilation by ion impact is approximately 85 nm^2. Crater formation is not, in general, accompanied by the emission of crater-sized particles although occasionally (≈ 1 per 2000 craters) such a particle is emitted from the surface. Crater creation and ion-induced annihilation result from radiation-induced flow associated with energy spikes.

The processes observed here may also be involved in other interface phenomena occurring in gold and other high-Z, or high-density metals under ion irradiation. These include the development of surface topography, grain-boundary movement, ion-beam mixing and gas bubble and precipitate behavior under ion irradiation. As the creation of a crater may involve tens of thousands of atoms, the single-ion induced, pulsed localized flow process reported here may be the most significant mechanism in determining the interface behavior of dense high Z metals under irradiation.

ACKNOWLEDGMENTS

We wish thank B. Kestel for specimen preparation, R. E. Cook for assistance with analytical measurements, and E. Ryan, L. Funk, T. McCormick, P. M. Baldo, and S. Ockers for assistance with the *in situ* TEM experiments. This work has been supported by the U.S. Department of Energy, BES-Materials Sciences, under Contract No. W-31-109-Eng-38 and by a collaborative research Grant No. 910670 from NATO. S.E.D. acknowledges funding from the Materials Science Division at Argonne National Laboratory.

*On leave from Joule Physics Laboratory Science Research Institute, University of Salford, Salford M5 4WT, United Kingdom.

[1] J. A. Brinkman, J. Appl. Phys. **25**, 951 (1954).
[2] J. A. Brinkman, Am. J. Phys. **24**, 246 (1956).
[3] K. L. Merkle and W. Jâger, Philos. Mag. A **44**, 741 (1981).
[4] J. A. Davies, G. Foti, L. M. Howe, J. B. Mitchell, and K. B. Winterbon, Phys. Rev. Lett. **34**, 1441 (1975).
[5] D. A. Thompson and S. S. Johar, Appl. Phys. Lett. **34**, 242 (1979).
[6] H. H. Andersen and H. L. Bay, J. Appl. Phys. **46**, 2416 (1975).
[7] S. E. Donnelly, R. C. Birtcher, C. Templier, and V. Vishnyakov, Phys. Rev. B **52**, 3970 (1995).
[8] R. C. Birtcher and S. E. Donnelly, Phys. Rev. Lett. **77**, 4374 (1996).
[9] C. W. Allen, L. L. Funk, E. A. Ryan, and S. T. Ockers, Nucl. Instrum. Methods Phys. Res. B **40/41**, 553 (1989).
[10] T. S. Lin and Y. W. Chung, Surf. Sci. **207**, 539 (1989).
[11] G. Betz and W. Husinsky, Nucl. Instrum. Methods Phys. Res. B **102**, 281 (1995).
[12] J. F. Ziegler, J. P. Biersak, and U. Littmark, *The Stopping and Ranges of Ions in Solids* (Pergamon, New York, 1985).
[13] R. S. Averback, M. Ghaly, and H. Zhui, in *Microstructures of Irradiated Materials*, edited by I. M. Robertson *et al.*, MRS Symposia Proceedings No. 373 (Materials Research Society, Pittsburgh, 1995), p. 3.
[14] G. W. Greenwood, A. J. E. Foreman, and D. E. Rimmer, J. Nucl. Mater. **4**, 305 (1959).
[15] D. J. Bacon and T. Diaz de la Rubia, J. Nucl. Mater. **216**, 275 (1994).